Geoid
Journal of Geodesy and Geomatics

Geoid Vol. 20, No. 2, 2025, 22-34

P-ISSN: 1858-2281; E-ISSN: 2442-3998

Development of Three.js-based 3D Scenes with Seamless Visualisation of Gaussian Splatting and Transformation to Global Coordinates

Azfa Ahmad Dzulvikar*[1], Harintaka[1], Ikhrom[2]
[1]Geodetic Engineering Department, Faculty of Engineering, Universitas Gadjah Mada, Yogyakarta, 55281, Indonesia
[2]Universitas Islam Negeri Walisongo, Semarang, 50185, Indonesia
*Corresponding author: azfaahmaddzulvikar@mail.ugm.ac.id

Received: 04 June 2025; Revised: 02 October 2025; Accepted: 05 October 2025; Published: 05 October 2025

Abstract: Existing scholarly literature on the Gaussian Splatting algorithm has predominantly concentrated on improving the rendering and reconstruction of three-dimensional objects, as well as exploring its applications in various academic disciplines, such as medicine, robotics, and mapping, while being limited to local coordinate systems. This study describes the development of a 3D scene modelled using the Gaussian Splatting algorithm, featuring accurate distance and position geometry based on three.js. The developed 3D scene was then evaluated with precise position and distance coordinates in the field and compared to the established SfM-MVS (Structure from Motion-Multi View Stereo) algorithm. The findings demonstrate that the proposed development successfully generated three.js-based 3D scenes with global coordinate compatibility, utilising the Gaussian Splatting algorithm, achieving the same level of position and distance accuracy as the SfM-MVS algorithm, with a 95% confidence level using a T-test. This research concludes that the developed approach is successful and can be further expanded for various scientific fields that require accurate position and distance information using the Gaussian Splatting Algorithm.

Keywords: Distance Geometry, Gaussian Splatting, Position, three.js, SfM-MVS

How to cite: Dzulvikar, A.A., HArintaka, Ikhrom. (2025). Development of Three.js-based 3D Scenes with Seamless Visualisation of Gaussian Splatting and Transformation to Global Coordinates. *Geoid, 20*(2), 22-34.

Introduction

Over the past several years, three-dimensional modelling approaches have garnered substantial attention and application across diverse academic disciplines, encompassing domains such as computer vision and geospatial analysis (Karnawat et al., 2023). The Gaussian Splatting algorithm remains a prominent approach in the field of three-dimensional modelling, even with the emergence of more recent techniques such as Neural Radiance Field (NeRF) (Mildenhall et al., 2022; Petrovska et al., 2023; Rabby and Zhang, 2023; Tancik et al., 2023; Warburg et al., 2023). This method represents 3D scenes through the utilisation of a collection of three-dimensional Gaussian distributions, where each Gaussian distribution is defined by a position vector and a covariance matrix (Kerbl et al., 2023). This enables the Gaussian Splatting algorithm to generate detailed and comprehensive three-dimensional scenes while maintaining a smaller file size and reduced computational requirements.

Recent studies examining the Gaussian Splatting algorithm have predominantly focused on improving the rendering (Fei et al., 2024; Kerbl et al., 2023; Luo et al., 2024; Matsuki et al., 2023) and reconstruction (G. Chen and Wang, 2024; Malarz et al., 2023; Qin et al., 2023; Wu et al., 2024) of three-dimensional objects, in addition to its utilization across various fields including medical (Y. Chen and Wang, 2024; Liu et al., 2024), robotics (Fei et al., 2024; Matsuki et al., 2023), and mapping, while still employing local coordinate systems (Fei et al., 2024; Luo et al., 2024; Matsuki et al., 2023). Existing literature has not explored the application of the Gaussian Splatting algorithm to generate 3D scenes with accurate global coordinates above the Earth's surface. This capability could hold great potential, as the Gaussian Splatting method's ability to create lightweight, high-fidelity 3D models could solve many problems requiring precise position and distance

information in global coordinate systems.

To address this gap, this study aims to develop a three.js-based 3D scene that leverages the Gaussian Splatting algorithm to achieve accurate distance and position geometry. The methodology involves the development of a viewer system, built upon the three.js library, to render 3D scenes generated via the Gaussian Splatting algorithm. Accurate georeferencing is achieved through the integration of external transformation data obtained from Structure-from-Motion software, consistent with the approach described by Tavani et al. (2014), ensuring the establishment of precise global coordinates before the Gaussian Splatting process. The developed approach undergoes rigorous validation via empirical field testing and comprehensive statistical analysis, with performance benchmarked against the established SfM-MVS method. This comparative assessment, consistent with validation methodologies employed in prior scholarly research (Apriansyah and Harintaka, 2023a, 2023b; Balloni et al., 2023; Condorelli et al., 2021; Elkhrachy, 2021; Hillman et al., 2021; Kovanič et al., 2023; Li et al., 2024; Mandaya, 2020; Mokroš et al., 2021; Murtiyoso et al., 2024; Negara and Harintaka, 2021; Petrovska et al., 2023; Xie et al., 2023; Zainuddin et al., 2024; Zhou et al., 2022), aims to ascertain and confirm the accuracy of both positional and distance geometry.

In assessing positional accuracy for geospatial data, two primary metrics are used: Circular Error at 90% confidence level (CE90) and Linear Error at 90% confidence level (LE90), which refer to the regulation of Badan Informasi Geospasial (2018). CE90 quantifies horizontal accuracy, defining the radius within which 90% of horizontal positions are anticipated to lie. Conversely, LE90 represents vertical accuracy, delineating the elevation error range encompassing 90 percent of the data points. Complementing positional accuracy evaluation, statistical validation is performed using the T-test. The T-test, a parametric statistical method, facilitates the determination of statistically significant differences between data sets (Gaussian Splatting with SfM-MVS), provided that the data first meet the assumptions of normal distribution as described by Ghilani (2017). A more detailed exposition on the application of Independent Check Points (ICP) for CE90 and LE90 assessment, alongside the methodologies of the T-test, is provided within the Data and Method section.

The key objectives of this research are: 1) to develop a system capable of conveniently displaying 3D scenes generated using the Gaussian Splatting algorithm and transforming them from local to global coordinates on the Earth's surface; and 2) to evaluate the results of 3D scenes converted to global coordinates through field data assessment and statistical comparison to the previous SfM-MVS algorithm. This study hypothesises that the development of a 3D scene viewer using three.js will result in 3D scenes with accurate geometry and object positions on the Earth's surface.

Data and Method

The Tugu Temple in Semarang City was selected as the case study site due to its varied colours and straightforward geometric structure, which are beneficial for assessing positional and distance accuracy. This project also serves the secondary objective of documenting this historically significant but less widely recognised cultural heritage site. The temple, situated on Tugurejo, Tugu District, Semarang City, Central Java, with geographic coordinates of approximately -6.980 latitude and 110.349 longitude, was digitally captured via aerial photography utilising a DJI Phantom 4 drone. To facilitate accurate spatial referencing, the site was equipped with four control points and three check points, the precise coordinates of which were meticulously determined through integrated Global Navigation Satellite System (GNSS) and Total Station (TS) surveying techniques. Specifics on the spatial positioning of these points and the process for validating distances are presented in Figure 1, while the dataset utilised in this study is presented in Table 1. Specifics on the spatial positioning of these points and the process for validating distances are presented in Figure 1, while the dataset utilised in this study is presented in Table 1.

Data collection for this research was facilitated by three primary instruments possessing relevant technical specifications. For aerial data acquisition, a DJI Phantom 4 drone equipped with a 12.4-megapixel CMOS sensor camera was utilised. The measurement of control and check point coordinates in the field was conducted

using two types of geodetic Global Navigation Satellite System receivers: Topcon Hiper SR and Hiper II, both capable of tracking signals from multiple satellite constellations for high precision. Subsequently, for distance and position determination requiring millimetre accuracy, a Sokkia IM-52 Total Station was employed, featuring a 2-arcsecond angular accuracy and a reflectorless distance measurement capability up to 500 meters.

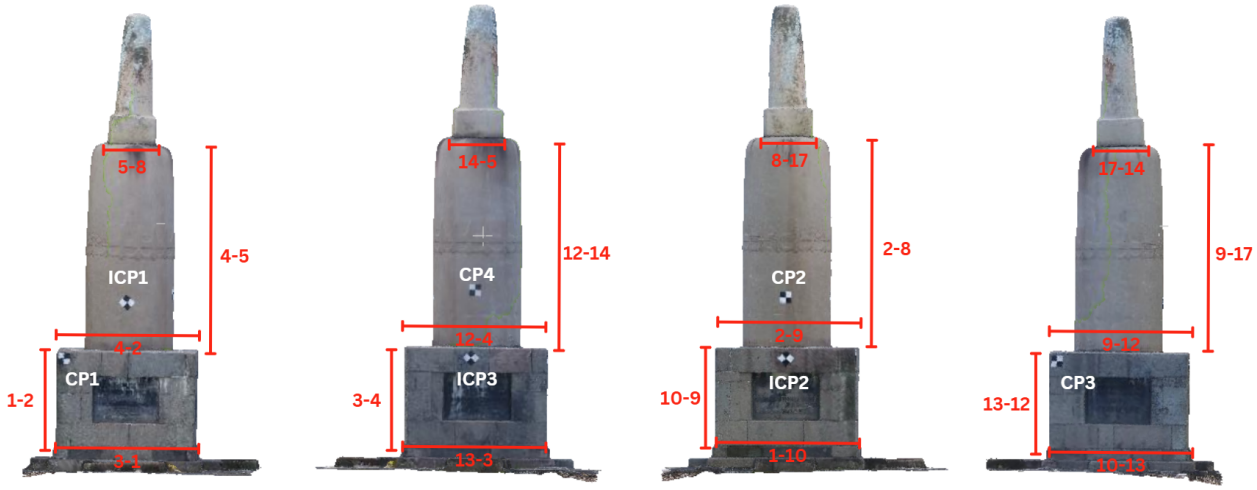

Figure 1. CP (Control Points) Position for Model Binding, ICP (Independent Check Points) for Position Geometry Accuracy Testing, and Test Distance Position for Distance Geometry Accuracy Testing

Table 1. The Dataset Used in This Study

No	Data	Sources
1	Object photo of Tugu Temple	DJI Phantom 4
2	Control Point Coordinates	GNSS and TS
3	Check Point Coordinates	GNSS and TS
4	Object Distance Data	GNSS and TS

The required equipment comprises: 1) SfM based software for processing aligned photographs, which are bound to control points to obtain camera pose data in the georeferenced COLMAP txt format, as well as marker data to obtain transformation information; 2) The Gaussian Splatting processing software, Jawset Postshot, was employed with the exported camera pose data; 3) Basic software for developing web-based applications, such as Laravel or a similar platform; 4) The three.js library, accessible from GitHub repository at Kellog (2025) and mrdoob (2024).

The study is structured in three phases: 1) The preparatory phase, encompassing data preparation and application development; 2) The processing phase, which includes SfM-MVS processing in SfM-based software, Structure from Motion-Gaussian Splatting (SfM-GS) processing utilising SfM-based software-Jawset Postshot, and the evaluation of model results within the developed application using validation data; 3) The final phase, involving the analysis of position accuracy, distance accuracy, and application development result performance. The three phases can be seen in full in Figure 2.

This preparatory phase involves compiling control point and checkpoint data, obtained through GNSS and total station surveying techniques, into an Excel format. Parallel research endeavours have implemented similar processes (Balloni et al., 2023; Condorelli et al., 2021; Kovanič et al., 2023; Mokroš et al., 2021; Morita et al., 2024; Murtiyoso et al., 2024; Petrovska et al., 2023; Xie et al., 2023; Zhou et al., 2022), involving the preparation of distance data derived from GNSS and total station measurements, in conjunction with a photographic dataset documenting the temple structure. The subsequent step consists of developing a three.js-based application that leverages resources from the GitHub repositories referenced in Kellogg (2025) and mrdoob (2024). The specifics and implementation details of the software development process can be accessed through these sources Dzulvikar (2025).

The second stage, the processing phase, commences with Structure-from-Motion processing. This involves associating control points within each photograph using SfM-based software, enabling the acquisition of camera pose data in the COLMAP format. Furthermore, marker data is obtained, providing detailed information regarding the transformation from local to global coordinate systems on the Earth's surface, a methodology consistent with that employed by Tavani et al. (2014) to derive camera pose and transformation data. The subsequent processing can be divided into several steps: 1) The workflow initiates with the Structure-from-Motion pipeline, proceeding to the Multi-View Stereo stage, ultimately resulting in the creation of a georeferenced mesh model. This approach is consistent with methodologies employed in prior research (Condorelli et al., 2021; L. Gao et al., 2022; Gómez-Gutié Rrez et al., 2015), wherein comparable workflows are utilised to generate georeferenced mesh models; 2) The second step involves a Gaussian Splatting process in Jawset Postshot, using four key data sources from the camera pose data - namely, cameras.bin, images.bin, points3D.bin, and all Tugu temple images. The resulting 3D scene remains in the local coordinate system, a method that has also been utilized in similar studies (Abramov et al., 2024; Previtali et al., 2024; Sannholm, 2024); 3) Thirdly, the SfM-MVS model can be directly evaluated using position and distance geometry test data with generalized Root Mean Square Error as outlined in Badan Informasi Geospasial (2018) and T-test methods, consistent with implementations detailed in the research of Cahyono and Pratomo (2008), Pham et al. (2023), and Usud and Sukojo (2014). In contrast, the SfM-GS model is integrated into the developed application alongside XML-formatted transformation data, and the same assessment is conducted as on the SfM-MVS model.

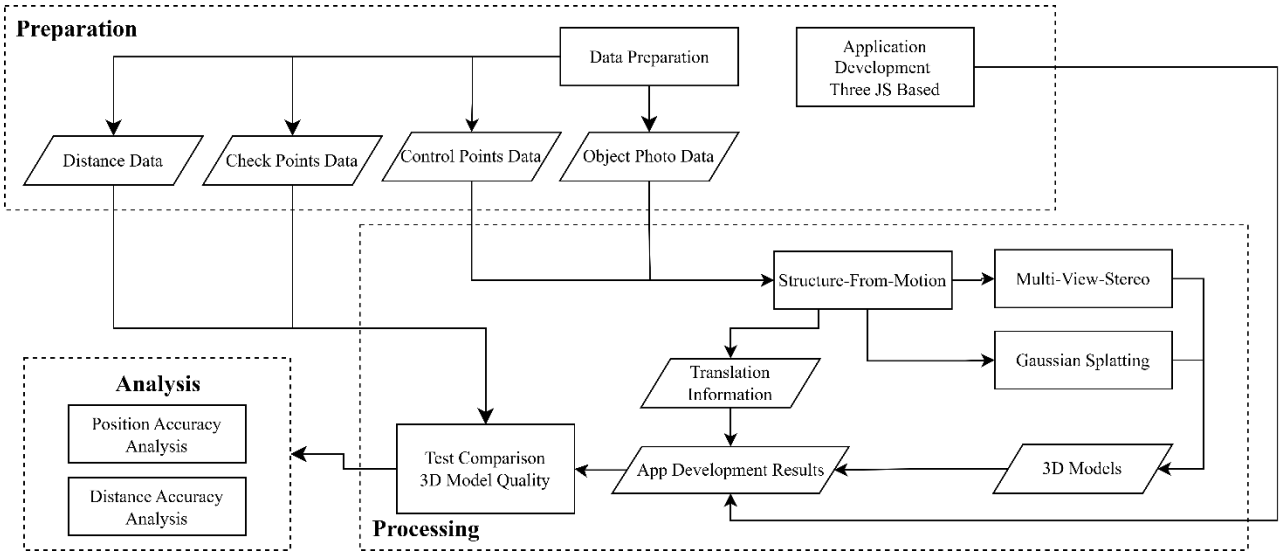

Figure 2. Research Flow Chart

The validation design further encompasses an examination of the developed system's positional accuracy through CE90 and LE90 metrics, signifying horizontal and vertical accuracy standards, respectively. These metrics are ascertained utilising ICP as validation data, adhering to the technical specifications for spatial data accuracy outlined in the Head of the Geospatial Information Agency Regulation Number 6 of 2018 (Badan Informasi Geospasial, 2018), thereby establishing the benchmark for acceptable positional accuracy in alignment with national geospatial standards. The calculation of CE90 and LE90 generally involves multiplying the root mean square error values for the horizontal and vertical position components by their corresponding statistical factors to establish error limits at a 90% confidence level, as detailed by Badan Informasi Geospasial (2018). Additionally, a statistical validation is performed via a T-Test, a parametric statistical methodology, to ascertain whether the Gaussian Splatting model exhibits positional and geometric accuracy comparable to the established SfM-MVS model, which serves as the reference dataset. This comparison aims to determine the statistical equivalence of the Gaussian Splatting model's accuracy to that of the SfM-MVS method.

Before conducting the T-test, a normality test is executed, as the T-test assumes normally distributed data. Data is deemed normally distributed if the computed Dmax value (the highest difference sample data value) is less than the Lilliefors distribution normal test critical value, L-Table, which is determined by the sample size and significance level or confidence level (Ghilani, 2017). This criterion signifies that the data does not exhibit a substantial departure from a normal distribution. Subsequently, the T-test is performed, wherein the null hypothesis posits no statistically significant disparity between the two datasets. For the null hypothesis to be accepted, the t-value must have a value inside the t-table interval area (Ghilani, 2017). A confidence level of 95% is commonly employed, reflecting a consensus within the scientific community that it strikes a reasonable balance between precision and the risk of erroneously concluding an effect exists (Ghilani, 2017). A t-value located outside the t-table interval area suggests that any observed difference between the SfM-GS and SfM-MVS datasets is attributable to random variation rather than a genuine divergence in their geometric accuracy. This thorough methodology guarantees that the outcomes derived from the Gaussian Splatting process are not only positionally precise but also statistically substantiated in comparison to an established methodology. This method is akin to the approach undertaken by Cahyono and Pratomo (2008) and Usud and Sukojo (2014).

Currently, no regulations specifically standardise the positional accuracy and distance geometry for 3D models generated using non-metric photogrammetry methods. Existing positional accuracy standards, such as those published by ASPRS, are primarily intended for metric photogrammetry and do not explicitly address non-metric techniques, particularly those employing convergent object photo acquisition. To address this standardisation gap, this study adopts an alternative validation approach. This involves applying general spatial data accuracy standards from the Regulation of the Head of the Geospatial Information Agency and performing a statistical T-test on the Structure-from-Motion-Multi-View-Stereo algorithm, which is widely recognised as a benchmark in non-metric photogrammetry.

The efficacy of the developed three.js-based 3D viewer in accurately transforming Gaussian Splatting models to global Earth coordinates was assessed using simple validation criteria. The developed system is deemed unsuccessful or inaccurate if its testing results reveal a significant difference in positional accuracy metrics (CE90 and LE90) when compared to the reference SfM-MVS model. This conclusion is further reinforced statistically if the T-test indicates a significant difference between the two algorithms, leading to the rejection of the null hypothesis at the predetermined significance level.

Results and Discussion

Application Development Results

The study has successfully developed an application that integrates Gaussian Splatting, a technique originally designed for local coordinate rendering, into a system capable of precise geospatial representation. This achievement demonstrates the versatility of Gaussian Splatting and its potential for broader applications beyond its initial scope. The development details, rendering techniques, and programming structure of the developed system have been thoroughly documented in the Github documentation Dzulvikar (2025), with links provided allowing readers to learn and implement this development and further examine the system for future studies.. As illustrated in Figure 3, the results of the application development are presented. The developed application incorporates capabilities for transforming data from local to global coordinate systems, leveraging XML-formatted external transformation information. Furthermore, it includes functionalities enabling the measurement of points, distances, and areas in metric units. These features are designed to facilitate the assessment of model position and distance geometry accuracy.

A key advantage of the developed application is its capacity for efficient compression of 3D scene files. The transformation from the PLY (Polygon File Format) format to the compressed splat format (KSplat) is demonstrated by Kerbl et al. (2023). The KSplat format application achieves substantially reduced file sizes in comparison to both the original dataset and the traditional SfM-MVS approach. Notably, despite this significant reduction in file size, the visual quality and level of detail of the Gaussian Splatting-based 3D scene remain preserved, ensuring an optimal balance between storage efficiency and high-fidelity visualisation. This

compression capability directly contributes to the application's fast loading times and smooth rendering performance, mitigating the delays typically encountered when handling large 3D datasets.

The successful implementation of the efficient compression and global coordinate transformation validates the effectiveness of the developed application. The ability to quickly load and display complex 3D scenes from the Gaussian Splatting technique without noticeable quality degradation confirms that this approach is both practical and scalable for web-based geospatial applications. This finding addresses the primary challenge of integrating Gaussian Splatting into real-world geospatial systems, demonstrating that it can be utilised effectively without excessive computational overhead or long processing times. Consequently, this development represents a significant advancement in making Gaussian Splatting a viable alternative for large-scale 3D mapping, visualisation, and spatial analysis.

Figure 3. The Appearance of the 3DGS Viewer Development Results

Analysis of Position Geometry Accuracy

Evaluating the geometric positional accuracy is essential in Structure-from-Motion techniques, particularly when comparing the efficacy of the SfM-GS and SfM-Multi-View Stereo methods. The assessment utilising CE90 and LE90 metrics provides a thorough understanding of their spatial accuracy. The results indicate notable variations in positional precision, which are subsequently analysed. The visual representation of the position geometry accuracy analysis is presented in Figure 4. The results suggest that SfM-MVS provides significantly lower errors and higher positional accuracy compared to SfM-GS.

A comparative analysis reveals substantial differences in positional accuracy between the SfM-GS and SfM-MVS methods. The total horizontal error for SfM-GS is 0.41 mm, significantly higher than the 0.01 mm observed for SfM-MVS. A similar trend is observed for the vertical total mistake, with SfM-GS showing 5.23 mm compared to a considerably lower 0.14 mm for SfM-MVS. These findings indicate that the SfM-MVS approach provides slightly more consistent and precise geospatial reconstructions than the SfM-GS technique.

The Root Mean Square Error (RMSE) values further confirm the slightly superior positional accuracy of the SfM-MVS approach compared to SfM-GS. For SfM-GS, the RMSE values for the horizontal and vertical components are 11.66 mm and 41.76 mm, respectively. In contrast, SfM-MVS reported significantly lower RMSE values, at 1.81 mm and 6.95 mm, respectively. These findings indicate that the SfM-MVS method is more effective in minimising spatial deviation, thus ensuring higher precision in 3D reconstruction applications.

The average error provides insight into the average deviation of the reconstructed model from the actual reference point. The analysis shows that the average horizontal error for the SfM-GS approach is 0.14 mm, while the error for the SfM-Multi-View Stereo method is much lower at 3.3 µm. Similarly, the average vertical error for SfM-GS is 1.74 mm, while SfM-MVS achieves a lower average vertical error of 0.05 mm. These findings indicate that the SfM-MVS technique maintains a slightly higher level of geometric accuracy in both the horizontal and vertical dimensions.

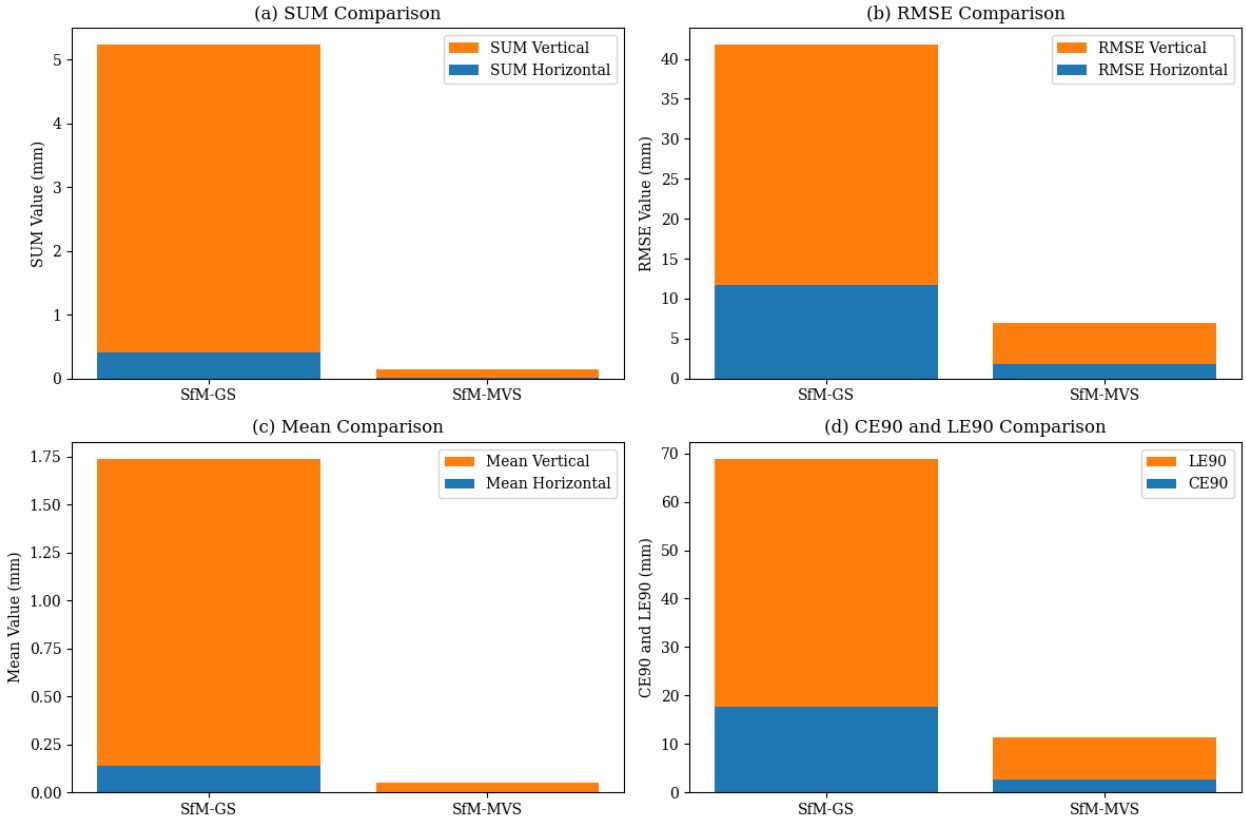

Figure 4. Comparison of geometric positional accuracy between SfM-GS and SfM-MVS

The CE90 and LE90 metrics provide a 90% confidence level for horizontal and vertical positional accuracy, respectively. Analysis shows that the SfM-GS approach exhibits a CE90 of 17.70 mm and an LE90 of 68.90 mm, while the SfM-MVS method records a significantly lower CE90 of 2.74 mm and an LE90 of 11.46 mm. These findings further validate that the SfM-MVS technique provides slightly better positional accuracy with a higher degree of confidence in the spatial alignment of the reconstructed model.

The discrepancies in geometric precision between the two methods are attributable to their respective computational paradigms. SfM-GS, predicated on Gaussian Splatting, employs a probabilistic density estimation approach to delineate the 3D structure, a methodology with precedent in prior research (G. Chen and Wang, 2024; Fei et al., 2024; Kerbl et al., 2023; Liu et al., 2024; Luo et al., 2024; Malarz et al., 2023; Matsuki et al., 2023; Qin et al., 2023; Wu et al., 2024). While the Gaussian Splatting method offers adaptability in rendering complex scenes, it may introduce spatial inconsistencies, especially in intricate geometric reconstructions. In contrast, the Structure-from-Motion with Multi-View Stereo approach employs a dense stereo matching algorithm, which refines feature correspondences and diminishes uncertainties in spatial localization, as evidenced in prior studies (Balloni et al., 2023; Condorelli et al., 2021; Elkhrachy, 2021; Hillman et al., 2021; Kovanič et al., 2023; Li et al., 2024; Mokroš et al., 2021; Murtiyoso et al., 2024; Petrovska et al., 2023; Xie et al., 2023; Zainuddin et al., 2024; Zhou et al., 2022). The deterministic nature of MVS ensures enhanced accuracy and robustness to environmental variations, rendering it a more reliable methodology for precise 3D modelling.

Moreover, the extant literature indicates that surface texture and lighting conditions exert influence on accuracy (Karnawat et al., 2023; Kerbl et al., 2023; Morita et al., 2024; Tang et al., 2023; Zainuddin et al., 2024; Zhao et al., 2024). The reliance of Gaussian Splatting on probabilistic estimation makes it more sensitive to variations in input data. In contrast, MVS maintains structural consistency across diverse lighting and texture conditions, contributing to its improved performance.

These findings clearly indicate that the SfM-MVS approach slightly outperforms the SfM-GS method in terms of geometric accuracy. However, it is crucial to recognise that both techniques achieve precision at the centimetre scale, which is already considered highly accurate for many geospatial applications in prior studies (Barba et al., 2019; El Barhoumi et al., 2022; S. Gao et al., 2022; McDermott and Rife, 2024). This level of precision represents a significant advancement, enabling reliable 3D modelling and spatial mapping in real-world scenarios. Although the SfM-MVS approach demonstrates marginally superior performance, the ability of the SfM-GS method to maintain accuracy at such a granular level is a significant accomplishment. This offers considerable flexibility for applications where the absolute highest precision is not an essential criterion. These results provide valuable insights for professionals and academics searching for computationally efficient and adaptable methodologies in geospatial modelling. Additionally, the statistical outcomes derived from the ICP data are based on a limited sample size of four, necessitating further validation through a t-test capable of assessing the broader population.

Analysis of Distance Geometry Accuracy

To validate the necessary assumptions for parametric statistical analyses, the Lilliefors test was applied to both datasets to assess whether they exhibit a normal distribution, a method also employed by Ferreira et al. (2016) and Mbuli et al. (2022). As summarised in Table 2, the Dmax values for SfM-GS and SfM-MVS were found to be lower than their respective L-table values, confirming that both datasets conform to a normal distribution at a 95% confidence level. This finding is crucial, as it enables the use of the independent t-test to compare their mean geometric accuracy distances. The independent sample t-test was performed to investigate whether there was a statistically significant difference in geometric accuracy between the SfM-GS and SfM-MVS approaches. The analysis yielded a t-value of -0.80 and a t-table value of ±2.10, the results of which are illustrated by Figure 5. This finding indicates that the test fails to reject the null hypothesis, as the value of -0.80 lies between the two t-table values. This implies there is no statistically significant difference in geometric accuracy distance between the two methods at the 95% confidence level.

Table 2. Summary of Lilliefors and T-Test Results for Geometric Accuracy Distance

Statistic	Dmax	L Table	f(n)	t-value	t-table	Conclusion
SfM-GS Data	0.14	0.17	0.59			Data is normally distributed
SfM-MVS Data	0.11	0.17	0.49			Data is normally distributed
T-test				-0.80	±2.10	Fail to reject H0, no significant difference

The results demonstrate that SfM-GS and SfM-MVS techniques achieve comparable geometric accuracy distances, despite their distinct computational frameworks. While SfM-MVS exhibits slightly more stability in the previous test, the findings confirm that SfM-GS remains a viable alternative with an equivalent mean geometric accuracy from the paired T-test. This discovery has important implications: 1) Both methods can be used interchangeably for applications requiring centimeter-level precision, such as topographic mapping, geospatial analysis, and 3D urban modeling, where centimeter-level accuracy is sufficient, as demonstrated by studies (Barba et al., 2019; El Barhoumi et al., 2022; S. Gao et al., 2022; McDermott and Rife, 2024); 2) Although in the previous test SfM-MVS had slightly better accuracy with three ICPs, in the paired T-test it was proven that SfM-GS had the same position and geometry accuracy as SfM-MVS in terms of population conditions with a 95% confidence level.

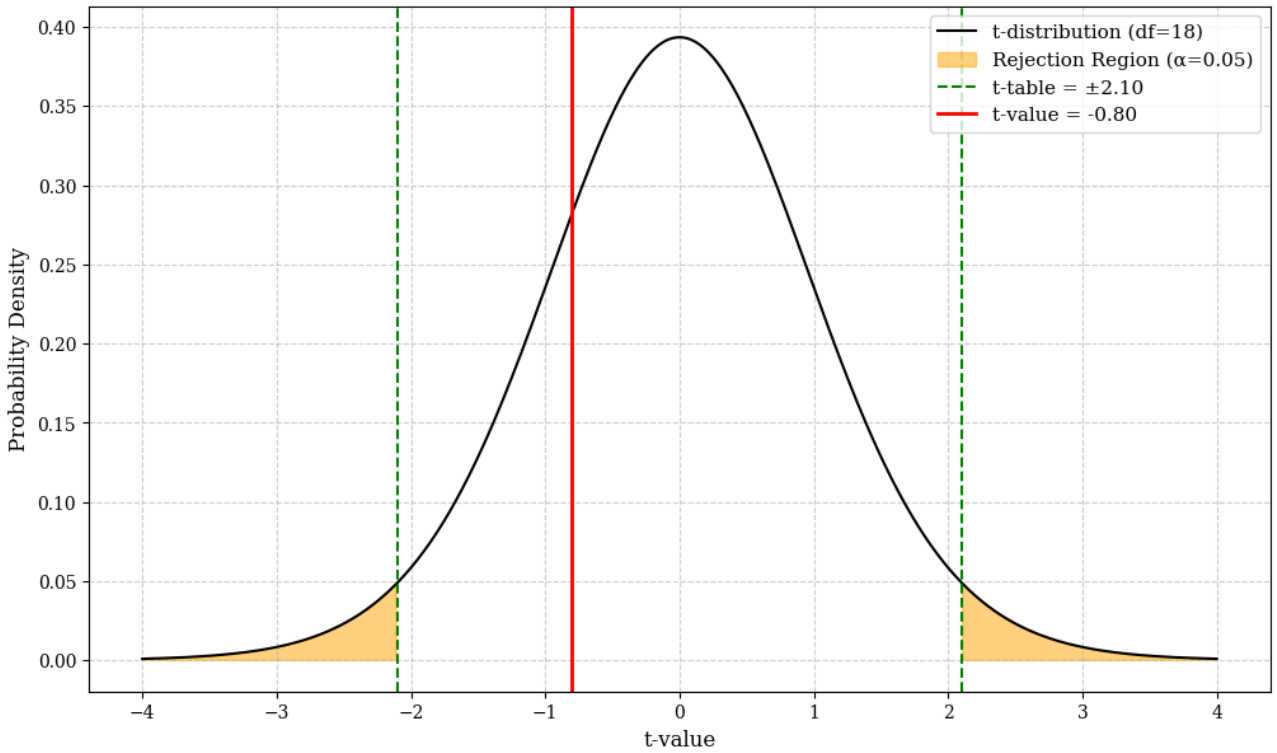

Figure 5. Illustration of T-Value and T-Table Position from Paired T-test

This research successfully demonstrates the integration of the Gaussian Splatting algorithm with global coordinate systems. The developed system enables the seamless visualisation of Gaussian Splatting-based 3D scenes and their transformation to global coordinates. Additionally, the study validates the reliability of the resulting position and distance geometry accuracy through field testing and statistical comparison to the established SfM-MVS algorithm. The findings show that the Gaussian Splatting approach achieves similar levels of position and distance accuracy as SfM-MVS in population conditions, with a 95% confidence level as determined by a T-test. This is supported by the null hypothesis being accepted, with the t-value being between the two t-tables. The next section of this study provides a detailed description of these key results.

This study confirms that Gaussian Splatting offers a compelling alternative to conventional Stereo Multi-View modelling, particularly in its ability to generate high-fidelity novel views efficiently. Despite this promise, a critical evaluation underscores several key limitations that must be overcome. First, the technique imposes heavy computational demands, requiring significant memory resources that scale with scene complexity, thereby limiting its application on consumer-grade hardware. Second, its accuracy is highly sensitive to lighting conditions; dynamic shadows or specular reflections can be misinterpreted, leading to visual artefacts. This sensitivity is more pronounced in uncontrolled outdoor environments than in stable indoor settings. Consequently, while Gaussian Splatting excels in controlled scenarios, its geometric fidelity can be less reliable in more complex, real-world conditions. Future work aimed at mitigating these computational and environmental constraints will be crucial for positioning this method as a more efficient and accurate successor to established 3D reconstruction techniques.

Conclusions

This research successfully established and confirmed a system capable of visualising 3D scenes generated through Gaussian Splatting, with accurate transformation into global coordinate systems. Employing both ICP analysis and a statistical T-test, the study demonstrated that this method achieves centimetre-level positional and geometric accuracy, exhibiting no statistically significant divergence from the benchmark SfM-MVS technique at a 95% confidence level. These outcomes position Gaussian Splatting as a potent alternative to

SfM-MVS, especially for applications necessitating efficient, real-time rendering. This opens avenues for practical deployment in fields such as interactive urban planning, the development of digital twins for infrastructure management, and the immersive documentation of cultural heritage sites through web-based platforms. While SfM-MVS may retain a marginal advantage in absolute positional accuracy, prospective research can address the existing limitations of Gaussian Splatting. To fully harness its capabilities, future endeavours should concentrate on optimising computational performance through techniques like splat pruning or quantisation for reduced memory usage and processing load, and enhancing geometric fidelity by incorporating explicit geometric constraints or surface priors into the training process to improve the reconstruction of intricate details and sharp edges. Through these advancements, Gaussian Splatting can mature into an increasingly efficient and accurate solution, reinforcing its significance in future geospatial applications.

Acknowledgment

The authors express gratitude to the developers of Jawset Postshot for providing the software used for Gaussian Splatting processing in this study. Acknowledgement is also given to Mark Kellogg and mrdoob for their contributions to the development of the 3DGS viewer through the three.js library. The authors further appreciate the developers of COLMAP for their SfM-MVS-based application, a valuable asset to this research. Finally, sincere thanks are extended to the laboratories within the Department of Geodetic Engineering at both Universitas Diponegoro and Universitas Gadjah Mada for the provision of essential equipment that supported this research endeavour.

References

Abramov, N., Lankegowda, H., Liu, S., Barazzetti, L., Beltracchi, C., and Ruttico, P. (2024): Implementing Immersive Worlds for Metaverse-Based Participatory Design through Photogrammetry and Blockchain, *ISPRS International Journal of Geo-Information*, 13(6). https://doi.org/10.3390/ijgi13060211

Apriansyah, M., and Harintaka (2023a): Pembuatan Model 3D Bangunan LoD3 Dengan Pemanfaatan Foto Udara dan Fotogrametri Terrestris Making 3D Building Models of LoD3 Using Aerial Photography and Terrestrial Photogrammetry, *Geoid: Journal of Geodesy and Geomatics*, 18(2), 243–252.

Apriansyah, M., and Harintaka, H. (2023b): Comparative Analysis of the Semantic Conditions of LoD3 3D Building Model Based on Aerial Photography and Terrestrial Photogrammetry, *Journal of Applied Geospatial Information*, 7(2), 927–931. https://doi.org/10.30871/jagi.v7i2.6634

Badan Informasi Geospasial (2018): Peraturan Kepala Badan Informasi Geospasial Nomor 6 Tahun 2018 Tentang Perubahan Atas Peraturan Kepala Badan Informasi Geospasial Nomor 15 Tahun 2014 Tentang Pedoman Teknis Ketelitian Peta Dasar, retrieved from internet: https://peraturan.bpk.go.id/Details/269444/peraturan-big-no-6-tahun-2018.

Balloni, E., Gorgoglione, L., Paolanti, M., Mancini, A., and Pierdicca, R. (2023): Few-shot photogrammetry: A comparison between nerf and mvs-sfm for the documentation of cultural heritage, *International Archives of the Photogrammetry, Remote Sensing and Spatial Information Sciences - ISPRS Archives*, International Society for Photogrammetry and Remote Sensing, 48, 155–162. https://doi.org/10.5194/isprs-Archives-XLVIII-M-2-2023-155-2023

Barba, S., Barbarella, M., Di Benedetto, A., Fiani, M., Gujski, L., and Limongiello, M. (2019): Accuracy assessment of 3d photogrammetric models from an unmanned aerial vehicle, *Drones*, 3(4), 1–19. https://doi.org/10.3390/drones3040079

Cahyono, D. T., and Pratomo, D. G. (2008): Analisa Hasil Pengamatan Pasang Surut Air Laut Metode Langsung dan Tidak Langsung, *Jurnal Geoid*, retrieved from internet: https://iptek.its.ac.id/index.php/geoid/article/view/6962, 3(2), 130–138.

Chen, G., and Wang, W. (2024): A Survey on 3D Gaussian Splatting, retrieved from internet: http://arxiv.org/abs/2401.03890, 1–20.

Chen, Y., and Wang, H. (2024): EndoGaussians: Single View Dynamic Gaussian Splatting for Deformable Endoscopic Tissues Reconstruction, retrieved September 17, 2024from internet: https://arxiv.org/abs/2401.13352v1.

Condorelli, F., Rinaudo, F., Salvadore, F., and Tagliaventi, S. (2021): A comparison between 3D reconstruction using nerf neural networks and MVS algorithms on cultural heritage images, *International Archives of the Photogrammetry, Remote Sensing and Spatial Information Sciences - ISPRS Archives*, 43, 565–570.

https://doi.org/10.5194/isprs-archives-XLIII-B2-2021-565-2021

Dzulvikar, A. A. (2025): 3DGS Georeferenced Viewer - Azfa Ahmad Dzulvikar, , retrieved March 6, 2025, from internet: https://github.com/masazfaa/tesisazfa-3DGSViewer/tree/main.

El Barhoumi, N., Hajji, R., Bouali, Z., Ben Brahim, Y., and Kharroubi, A. (2022): Assessment of 3D Models Placement Methods in Augmented Reality, *Applied Sciences (Switzerland)*, 12(20). https://doi.org/10.3390/app122010620

Elkhrachy, I. (2021): Accuracy Assessment of Low-Cost Unmanned Aerial Vehicle (UAV) Photogrammetry, *Alexandria Engineering Journal*, 60(6), 5579–5590. https://doi.org/10.1016/j.aej.2021.04.011

Fei, B., Xu, J., Zhang, R., Zhou, Q., Yang, W., and He, Y. (2024): 3D Gaussian Splatting as New Era: A Survey, *IEEE Transactions on Visualization and Computer Graphics*, PP(8), 1–20. https://doi.org/10.1109/TVCG.2024.3397828

Ferreira, J. E. V., Pinheiro, M. T. S., dos Santos, W. R. S., and Maia, R. da S. (2016): Graphical representation of chemical periodicity of main elements through boxplot, *Educacion Quimica*, 27(3), 209–216. https://doi.org/10.1016/j.eq.2016.04.007

Gao, L., Zhao, Y., Han, J., and Liu, H. (2022): Research on Multi-View 3D Reconstruction Technology Based on SFM, *Sensors*, 22(12). https://doi.org/10.3390/s22124366

Gao, S., Gan, S., Yuan, X., Bi, R., Li, R., Hu, L., and Luo, W. (2022): Experimental study on 3D measurement accuracy detection of low altitude uav for repeated observation of an invariant surface, *Processes*, 10(1). https://doi.org/10.3390/pr10010004

Ghilani, C. D. (2017): *Adjustment Computations*, *Adjustment Computations*, John Wiley & Sons, Inc. https://doi.org/10.1002/9781119390664

Gómez-Gutié Rrez, Á., Juan De Sanjosé -Blasco, J., Lozano-Parra, J., Berenguer-Sempere, F., De Matí As-Bejarano, J., Abellan, A., Jaboyedoff, M., Derron, M.-H., Kerle, N., and Thenkabail, P. S. (2015): Does HDR Pre-Processing Improve the Accuracy of 3D Models Obtained by Means of two Conventional SfM-MVS Software Packages? The Case of the Corral del Veleta Rock Glacier, *Remote Sensing 2015, Vol. 7, Pages 10269-10294*, 7(8), 10269–10294. https://doi.org/10.3390/RS70810269

Hillman, S., Wallace, L., Reinke, K., and Jones, S. (2021): A comparison between TLS and UAS LiDAR to represent eucalypt crown fuel characteristics, *ISPRS Journal of Photogrammetry and Remote Sensing*, 181(September), 295–307. https://doi.org/10.1016/j.isprsjprs.2021.09.008

Karnawat, K., Choudhari, H., Saxena, A., Singal, M., and Gadam, R. (2023): 3D reconstruction using Structure for Motion, retrieved August 7, 2024from internet: https://arxiv.org/abs/2306.06360v1.

Kellog, M. (2025): Releases · mkkellogg/GaussianSplats3D, , retrieved April 23, 2025, from internet: https://github.com/mkkellogg/GaussianSplats3D/releases.

Kerbl, B., Kopanas, G., Leimkuehler, T., and Drettakis, G. (2023): 3D Gaussian Splatting for Real-Time Radiance Field Rendering, *ACM Transactions on Graphics*, 42(4), 1–14. https://doi.org/10.1145/3592433

Kovanič, L., Štroner, M., Blistan, P., Urban, R., and Boczek, R. (2023): Combined ground-based and UAS SfM-MVS approach for determination of geometric parameters of the large-scale industrial facility – Case study, *Measurement: Journal of the International Measurement Confederation*, 216, 112994. https://doi.org/10.1016/j.measurement.2023.112994

Li, Q., Yang, G., Gao, C., Huang, Y., Zhang, J., Huang, D., Zhao, B., Chen, X., and Chen, B. M. (2024): Single drone-based 3D reconstruction approach to improve public engagement in conservation of heritage buildings: A case of Hakka Tulou, *Journal of Building Engineering*, 87(March), 108954. https://doi.org/10.1016/j.jobe.2024.108954

Liu, Y., Li, C., Yang, C., and Yuan, Y. (2024): EndoGaussian: Real-time Gaussian Splatting for Dynamic Endoscopic Scene Reconstruction, retrieved September 17, 2024from internet: https://arxiv.org/abs/2401.12561v2.

Luo, J., Huang, T., Wang, W., and Feng, W. (2024): A review of recent advances in 3D Gaussian Splatting for optimization and reconstruction, *Image and Vision Computing*, 151(May), 105304. https://doi.org/10.1016/j.imavis.2024.105304

Malarz, D., Smolak, W., Tabor, J., Tadeja, S., and Spurek, P. (2023): Gaussian Splatting with NeRF-based Color and Opacity, *Computer Vision and Image Understanding*, 251(July 2024), 104273. https://doi.org/10.1016/j.cviu.2024.104273

Mandaya, I. (2020): (Unmanned Aerial Vehicle) Untuk Identifikasi Dan Klasifikasi Jenis - Jenis Kerusakan Jalan, 14(3), 162–172.

Matsuki, H., Murai, R., Kelly, P. H. J., and Davison, A. J. (2023): Gaussian Splatting SLAM, retrieved from internet: http://arxiv.org/abs/2312.06741, 18039–18048.

Mbuli, N., Mendu, B., and Pretorius, J. H. C. (2022): Statistical analysis of forced outage duration data for subtransmission

circuit breakers, *Energy Reports*, 8, 1424–1433. https://doi.org/10.1016/j.egyr.2022.09.131

McDermott, M., and Rife, J. (2024): ICET Online Accuracy Characterization for Geometry-Based Laser Scan Matching, *Navigation, Journal of the Institute of Navigation*, 71(2). https://doi.org/10.33012/navi.647

Mildenhall, B., Srinivasan, P. P., Tancik, M., Barron, J. T., Ramamoorthi, R., and Ng, R. (2022): NeRF: Representing Scenes as Neural Radiance Fields for View Synthesis, *Communications of the ACM*, 65(1), 99–106. https://doi.org/10.1145/3503250

Mokroš, M., Mikita, T., Singh, A., Tomaštík, J., Chudá, J., Wężyk, P., Kuželka, K., Surový, P., Klimánek, M., Zięba-Kulawik, K., Bobrowski, R., and Liang, X. (2021): Novel low-cost mobile mapping systems for forest inventories as terrestrial laser scanning alternatives, *International Journal of Applied Earth Observation and Geoinformation*, 104, 102512. https://doi.org/10.1016/j.jag.2021.102512

Morita, M. M., Loaiza Carvajal, D. A., González Bagur, I. L., and Bilmes, G. M. (2024): A combined approach of SFM-MVS photogrammetry and reflectance transformation imaging to enhance 3D reconstructions, *Journal of Cultural Heritage*, 68, 38–46. https://doi.org/10.1016/j.culher.2024.05.008

mrdoob (2024): mrdoob/three.js: JavaScript 3D Library., retrieved February 8, 2025, from internet: https://github.com/mrdoob/three.js/.

Murtiyoso, A., Markiewicz, J., Karwel, A. K., Grussenmeyer, P., and Kot, P. (2024): Comparison of state-of-the-art multi-view stereo solutions for close range heritage documentation, *International Archives of the Photogrammetry, Remote Sensing and Spatial Information Sciences*, 48(2), 317–323. https://doi.org/10.5194/ISPRS-ARCHIVES-XLVIII-2-W4-2024-317-2024

Negara, T. B., and Harintaka (2021): Pemodelan Bangunan 3D Menggunakan Footprint Bangunan Hasil Ekstraksi Mask R-CNN dan Dense Point Cloud dari Foto Udara UAV, *Prosiding FIT ISI Vol 1, 2021 (248-260)*, 1, 248–260.

Petrovska, I., Jäger, M., Haitz, D., and Jutzi, B. (2023): Geometric Accuracy Analysis Between Neural Radiance Fields (NeRF) And Terrestrial Laser Scanning (TLS), *International Archives of the Photogrammetry, Remote Sensing and Spatial Information Sciences - ISPRS Archives*, Copernicus GmbH, 48, 153–159. https://doi.org/10.5194/isprs-archives-XLVIII-1-W3-2023-153-2023

Pham, H. T., Claessens, S., Kuhn, M., and Awange, J. (2023): Performance evaluation of high/ultra-high-degree global geopotential models over Vietnam using GNSS/leveling data, *Geodesy and Geodynamics*, 14(5), 500–512. https://doi.org/10.1016/j.geog.2023.03.002

Previtali, M., Barazzetti, L., and Roncoroni, F. (2024): Orthophoto generation with gaussian splatting : mitigating reflective surface artifacts in imagery from low-cost sensors, XLVIII(December), 12–13.

Qin, M., Li, W., Zhou, J., Wang, H., and Pfister, H. (2023): LangSplat: 3D Language Gaussian Splatting, 20051–20060. https://doi.org/10.1109/CVPR52733.2024.01895

Rabby, A. S. A., and Zhang, C. (2023): BeyondPixels: A Comprehensive Review of the Evolution of Neural Radiance Fields, *Journal of the ACM*, 37(111), 33. https://doi.org/https://doi.org/10.48550/arXiv.2306.03000

Sannholm, B. (2024): Real-Time Novel-View Synthesis for the Web Using 3D Gaussian Splatting Exploring Mesh-Supervised 3D Gaussian Scene Optimization and Efficient Web Rendering for Product Visualization, retrieved from internet: https://hdl.handle.net/2077/83678.

Tancik, M., Weber, E., Ng, E., Li, R., Yi, B., Kerr, J., Wang, T., Kristoffersen, A., Austin, J., Salahi, K., Ahuja, A., McAllister, D., and Kanazawa, A. (2023): Nerfstudio: A Modular Framework for Neural Radiance Field Development, *Proceedings - SIGGRAPH 2023 Conference Papers*. https://doi.org/10.1145/3588432.3591516

Tang, J., Zhou, H., Chen, X., Hu, T., Ding, E., Wang, J., and Zeng, G. (2023): Delicate Textured Mesh Recovery from NeRF via Adaptive Surface Refinement, *Proceedings of the IEEE International Conference on Computer Vision*, 17693–17703. https://doi.org/10.1109/ICCV51070.2023.01626

Tavani, S., Granado, P., Corradetti, A., Girundo, M., Iannace, A., Arbués, P., Muñoz, J. A., and Mazzoli, S. (2014): Building a virtual outcrop, extracting geological information from it, and sharing the results in Google Earth via OpenPlot and Photoscan: An example from the Khaviz Anticline (Iran), *Computers and Geosciences*, 63, 44–53. https://doi.org/10.1016/j.cageo.2013.10.013

Usud, A., and Sukojo, B. M. (2014): Analisis Pengaruh Tutupan Lahan Terhadap Ketelitian Aster Gdem V2 Dan Dem Srtm V4.1 (Studi Kasus: Kota Batu, Kabupaten Malang, Jawa Timur), *Geoid*, 10(1), 8. https://doi.org/10.12962/j24423998.v10i1.584

Warburg, F., Weber, E., Tancik, M., Holynski, A., and Kanazawa, A. (2023): Nerfbusters: Removing Ghostly Artifacts from Casually Captured NeRFs, *Proceedings of the IEEE International Conference on Computer Vision*, Institute of Electrical and Electronics Engineers Inc., 18074–18084. https://doi.org/10.1109/ICCV51070.2023.01661

Wu, T., Yuan, Y. J., Zhang, L. X., Yang, J., Cao, Y. P., Yan, L. Q., and Gao, L. (2024): Recent advances in 3D Gaussian

splatting, *Computational Visual Media*, 10(4), 613–642. https://doi.org/10.1007/s41095-024-0436-y

Xie, Y., Teo, M. X., Li, S., Huang, L., Liang, N., and Cai, Y. (2023): As-built BIM reconstruction of piping systems using smartphone videogrammetry and terrestrial laser scanning, *Automation in Construction*, 156, 105120. https://doi.org/10.1016/j.autcon.2023.105120

Zainuddin, K., Ghazali, M. D., Marzukhi, F., Samad, A. M., Ariff, M. F. M., and Majid, Z. (2024): Evaluation of nerf 3d reconstruction for rock art documentation, *International Archives of the Photogrammetry, Remote Sensing and Spatial Information Sciences - ISPRS Archives*, Copernicus GmbH, 48, 469–475. https://doi.org/10.5194/isprs-Archives-XLVIII-2-W4-2024-469-2024

Zhao, H., Zhao, X., Zhu, L., Zheng, W., and Xu, Y. (2024): HFGS: 4D Gaussian Splatting with Emphasis on Spatial and Temporal High-Frequency Components for Endoscopic Scene Reconstruction, retrieved September 17, 2024from internet: https://arxiv.org/abs/2405.17872v3.

Zhou, L., Meng, R., Tan, Y., Lv, Z., Zhao, Y., Xu, B., and Zhao, F. (2022): Comparison of UAV-based LiDAR and digital aerial photogrammetry for measuring crown-level canopy height in the urban environment, *Urban Forestry and Urban Greening*, 69(November 2021), 127489. https://doi.org/10.1016/j.ufug.2022.127489